Artifactual Inhomogeneities in Myocardial PET and SPECT Scans in Normal Subjects

Marissa L. Bartlett, Stephen L. Bacharach, Liisa-Maria Voipio-Pulkki and Vasken Dilsizian

Department of Nuclear Medicine, National Institutes of Health, Bethesda, Maryland and Department of Medicine, Turku University, Turku, Finland

It has been well established that PET and SPECT scans of human myocardium are subject to partial volume related effects, which can cause artifactual regional variations in activity around the myocardium. This study investigated the sources and magnitude of such artifactual inhomogeneity in subjects with normal cardiac function. **Method:** Using multi-slice, gated MRI scans from 9 normal subjects, we examined separately the influences on measured activity of wall motion, axial resolution and the relationship between wall thickness and in-plane resolution. **Results:** Two patterns of artifactual inhomogeneity were found: a depression in activity at the antero-apex and an elevation in activity in the free wall compared with the septum. Thus, in ungated PET images the true apical/septal ratio was artifactually reduced by a factor of 0.89 (0.92 for SPECT), while the true free wall/septal ratio was enhanced by a factor of 1.12 (1.19 for SPECT). Gating improved uniformity in end-systolic (ES) images but degraded uniformity in end-diastolic (ED) images. With gating, the true PET apical/septal ratio was artifactually reduced by only 0.97 at ES, and 0.82 at ED. Similar behavior was found for SPECT. Improvements in axial resolution were found to have little effect on artifactual variations. **Conclusion:** We find that the relationship between in-plane resolution and wall thickness, but not axial resolution, is of prime importance in determining the degree of artifactual inhomogeneity in ungated scans of normal human myocardium. Gating improved ES but degraded ED homogeneity.

Key Words: heart; emission computed tomography; artifacts; partial volume effect

J Nucl Med 1995; 36:188–195

PET scans of normal myocardium are commonly inhomogeneous, with regional variations in activity around the myocardium (*1,2*). Previous investigations suggest that the observed inhomogeneities are due, at least in part, to physiologic variations in uptake around the myocardium (*3,4*). However, other work has established that inhomogeneity of myocardial activity can also be caused by partial volume related effects, in both PET (*5*) and SPECT (*6*).

Received Feb. 17, 1994; revision accepted Aug. 1, 1994.

For correspondence and reprints contact: Dr. Marissa Bartlett, Dept. of Nuclear Medicine, National Institutes of Health, Bldg. 10, Room 1C401, Bethesda, MD 20892.

The purpose of this paper is to provide quantitative information about the effect of partial volume related inhomogeneities on tomographic scans of normal human myocardium. Use of gated cardiac MRIs enabled separate investigation of the different sources of partial volume related artifact-wall motion, axial resolution, variations in wall thickness and in-plane resolution. Thus, both the magnitude and genesis of these PET/SPECT artifactual inhomogeneities were quantitatively evaluated in normal subjects in noise-free images. The magnitude of these artifacts is important because it allows real physiologic variations to be distinguished from artifactual variations. The source of the artifacts is likewise important, in that it governs which properties of the imaging system bear most heavily on partial volume related nonuniformities in myocardial scans.

Together, information about the source and size of these partial volume artifacts has important implications for practical questions affecting myocardial scans. Such questions include: Does gating significantly reduce artifactual inhomogeneities? Is axial resolution a significant contributing factor to myocardial nonuniformity? Similarly, quantitative information about the relationship between in-plane resolution and wall thickening in normal humans will be useful in determining the impact on clinical scans of any improvement in in-plane resolution.

MATERIALS AND METHODS

To achieve the objectives of this study, it was necessary to obtain PET/SPECT images in which the myocardial concentration of radioactivity was known to be perfectly uniform. One approach would be to acquire images from normal subjects. However, it would not be possible to verify that the uptake in these subjects was indeed uniform and the acquired images would not yield information about the origin of any observed inhomogeneities. A second possible approach would be to use mathematical models of the myocardium. This approach also has a major flaw, in that the ability of such models to simulate reality is unknown. A third course was therefore chosen. Artificial PET/SPECT transaxial images were created from gated MRIs, using a technique previously applied to PET images of the brain (*7,8*). The resulting images are artificial only in the sense that the use of MRI data has allowed the underlying activity levels to be forced to be absolutely uniform. The cardiac anatomy, wall thickness, cardiac motion etc.—all the morphological features in space and time—are real measurements on normal subjects. Therefore, the partial volume

effects produced by these morphological features will be those actually occurring in the normal subjects studied.

Data Collection

Nine normal volunteers (7 males and 2 females) underwent MRI. All subjects were normal by history, physical examination and echocardiography. The average age was 27 yr (range 21–34 yr). Gated multislice spin echo MRIs were acquired on a 1.5 Tesla GE Signa with an echo time of 12–20 msec. Each subject's MRI data set consisted of 10 contiguous 10 mm thick slices, collected transaxially at 5 evenly spaced time points from end-diastole (ED) to end-systole (ES).

For each of the nine subjects, an MRI-based PET/SPECT central slice was created, visually located at the mid-cavity level of the left ventricle. In addition, MRI-based PET/SPECT slices were created at other levels of the heart: 10 mm more caudally (i.e., more apically) than the central slice and/or 10 mm more cephalad (i.e., closer to the base). Not all subjects had all three PET/SPECT slices created, because certain of the MRI slices were not of the very high quality necessary. Altogether, one central slice was produced in each of the nine subjects; a more basal slice was produced in seven of the subjects; and a more apical slice was produced in six of the subjects, resulting in 22 slices total.

Actual PET scans were also obtained in 5 of the 9 normal subjects using 5 mCi of ^{18}F-fluorodeoxyglucose (FDG). All subjects fasted overnight, and then received 50 g of glucose orally, 1 hr before the study. Static imaging began 30 min postinjection, and lasted 30 min. The PET data consisted of 21 transaxial slices, each separated by 5.1 mm, with an in-plane resolution of approximately 7 mm FWHM, and an axial resolution of 12.5 mm FWHM. The FDG scans were not gated.

Image Processing

MRIs (Fig. 1A) were used to create PET images with a known uniform underlying activity. Endocardial and epicardial regions of interest (ROIs) were drawn on each of the MRI transaxial slices of interest at each of the five time points (Fig. 1B). The pixel values between the endo- and epicardial borders (i.e., the myocardial pixels) were set to a value of 100 and all other pixels were set to a value of two. Thus, each MRI became an image of a perfectly uniform myocardium in a perfectly uniform background, with morphology accurately reflecting actual myocardial borders.

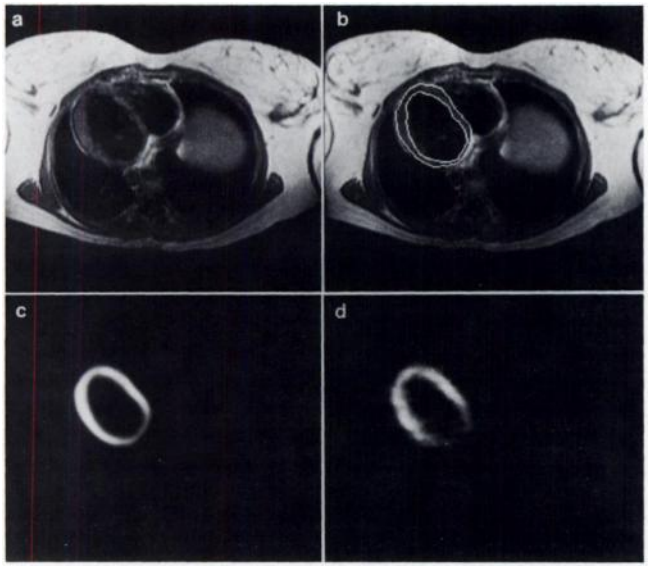

FIGURE 1. PET and SPECT images with a known uniform underlying activity were produced by using MRI (A) single MRI slice, (B) MRI slice with endo- and epicardial borders drawn, (C) MRI-based ungated PET image, and (D) actual corresponding FDG image.

To produce realistic PET images, the MRIs were appropriately blurred, spatially and/or temporally (as described below), to match the resolution characteristics of both high- and low-resolution PET scanners. Figure 1 (C and D) shows such an MRI-based PET image—in this case a noise-free version of an ungated image—and the corresponding actual FDG image. The two in-plane spatial resolutions investigated (7 mm and 14 mm FWHM) were chosen to span the range of reconstructed in-plane resolutions typically found in both recent and older PET scanners. In the same way, two axial resolutions were studied ("high" axial resolution and 12.5 mm FWHM axial resolution) which encompass the range of reconstructed axial resolutions typically obtained with both older and newer PET scanners. In addition, 14 mm in-plane resolution matches the typical in-plane resolution of myocardial SPECT imaging. Of course, the MRI-based images do not correspond to real SPECT images in that no attempt was made to reproduce the effects of scatter or photon attenuation. However, all the partial volume related effects investigated here apply to both PET and SPECT data. For simplicity, therefore, the images with low in-plane resolution will be referred to as SPECT images and those with high in-plane resolution will be referred to as PET images.

In all, three different types of resolution effects were considered: partial volume effects due to in-plane resolution, axial resolution and temporal resolution (i.e., wall motion and thickening). In-plane resolution was adjusted by blurring the data in-plane with a two-dimensional Gaussian filter. Similarly, axial blurring was performed by calculating an average of three contiguous MRI slices, weighted by a Gaussian with a FWHM of 12.5 mm (the resolution of the corresponding machines in our laboratory). Gaussian filters were used both in-plane and axially to match the resolution functions of a PET or SPECT imaging system, since most PET and SPECT scanners produce nearly Gaussian reconstructed point spread functions.

As noted above, as well as the 12.5-mm axial resolution, a "high" axial resolution was considered. The high axial resolution images were generated from a single MRI slice location. These MRI-based images had an axial resolution higher than the 10-mm MRI slice thickness because the myocardial edges were sharply defined by the endo- and epicardial ROIs.

Temporal blurring, to produce an ungated PET or SPECT image from a gated MRI data set, was performed by averaging the gated MRIs from different times throughout the cardiac cycle. The MRI data set contained only the time points from ED to ES. To create an accurate ungated image, images from time points later in the cardiac cycle were needed. To generate these, information was extracted from an average left ventricle (LV) volume curve obtained from ^{99m}Tc-labeled gated blood-pool scans of normal subjects. The fraction of time spent at each volume, as measured from the LV volume curve, determined weighting factors which were used to sum together the gated MR images. Therefore both gated and ungated (by appropriate summation of the gated data) MRI-based PET/SPECT images were produced. One representative subject is shown for PET resolution in Figure 2. The leftmost column shows the three slices for an ungated acquisition, while

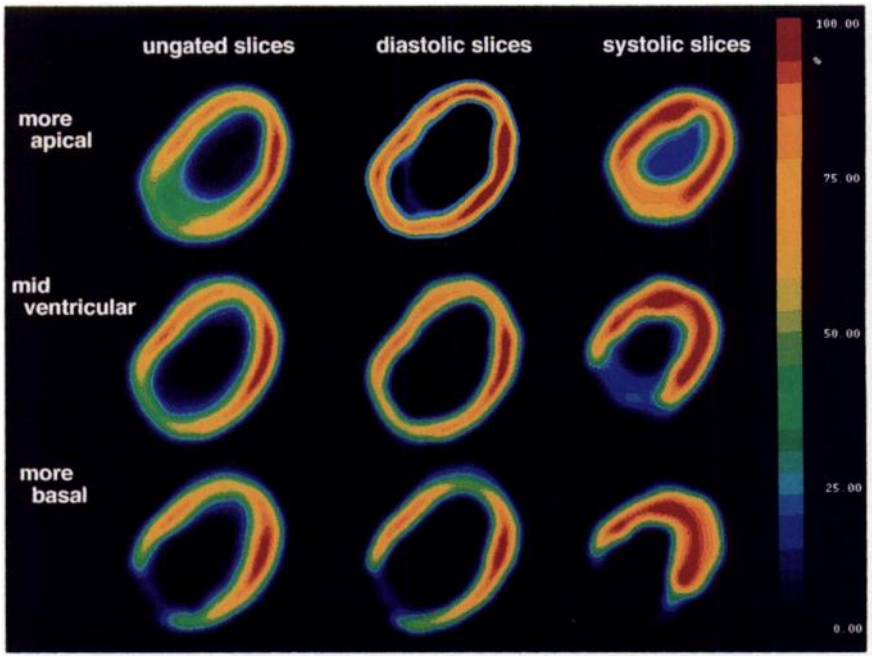

FIGURE 2. The MRI-based PET images with 12.5 mm axial resolution are shown for a single representative subject. Each row shows images from a different level in the heart. The columns (left to right) show ungated ED and ES images, respectively.

the middle and right columns show the gated images (12.5 mm axial resolution) at ED and ES.

In all, three types of images were considered: ungated images with 12.5-mm axial resolution; gated images with 12.5-mm axial resolution and gated images with "high" axial resolution. For all of these, both 7-mm and 14-mm in-plane resolution were considered.

Measurement of Activity

For each of the MRI-based PET and SPECT images, the myocardium was divided into 16 equal angle sectors, and the maximum of a myocardial profile across each sector was recorded. A myocardial profile is simply a record of the activity at a sequence of transmural points crossing the myocardium from just outside the epicardium to just inside the endocardium. A profile was generated for each sector by starting with an ROI markedly larger than the myocardium. The outer edge of the ROI was then successively shrunk towards the endocardial border, one line of pixels at a time (Fig. 3, left). The mean difference between pixel values in every pair of successively smaller ROIs constituted the profile (Fig. 3, right). The peak value of such a profile is a measure of the recovered activity of that sector. This technique is very similar to the widely used maximum circumferential profile method, except applied on a sector by sector basis.

RESULTS

The percent recovered activity was computed at each of the 16 sectors in the transaxial images by comparing the measured activity to the corresponding underlying true activity. The percent recovered activity at each sector was then averaged over the nine subjects for the three adjacent (more apical, mid-ventricular and more basal) slices to produce a plot of average percent recovered activity versus sector number (Fig. 4). (Note that this combination of adjacent slices is not the same as axial "blurring" of the slices—rather it simply lumps together the sector data extracted from similar anatomical regions at the three adjacent slice levels.) The sectors were numbered, with sectors 6 to 8 corresponding roughly to the anterior free wall, sectors 9 to 11 to the antero-apical area and sectors 12 to 14 to the anterior septum (Fig. 3). In the transaxial view, sectors 1, 2, 15 and 16 often encompassed the plane of the mitral valve, and the associated recovered activities were often very low (Fig. 4). These sectors were excluded from all calculations and will not be further discussed.

Patterns of Artifactual Inhomogeneity

The average percent recovered activity at each sector is plotted in Figure 4 (left side for PET resolution and right side for SPECT resolution). Visual observations from Figure 4 were quantified and tested for statistical significance. Specifically, the average recovered activity was

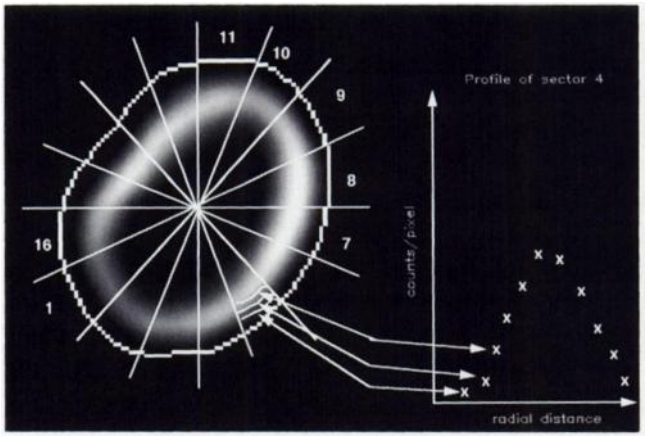

FIGURE 3. Shown on the left are three representative annular regions within a sector, produced by shrinking the original epicardial region. On the right, the mean counts per pixel in each of these annular regions is plotted against radial distance across the myocardium. The peak value of this profile was taken as the recovered activity.

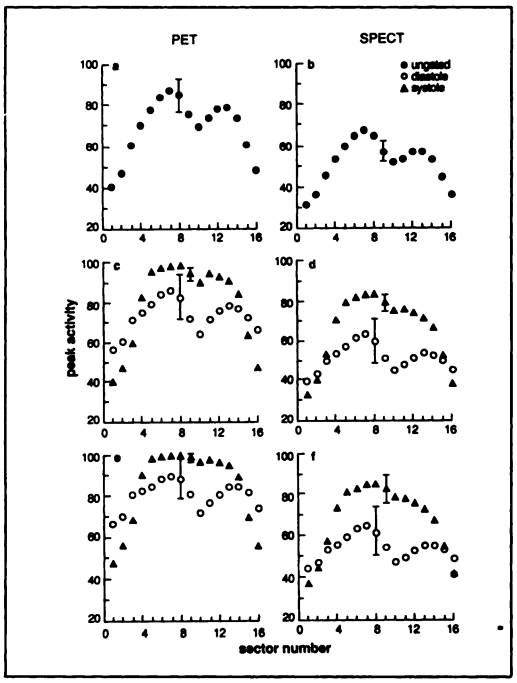

FIGURE 4. Average percent recovered activity at each sector: the left column of graphs show results for 7-mm in-plane resolution (PET) and the right column of graphs show results for 14-mm in-plane resolution (SPECT). The top row shows the ungated results (A and B), the middle row shows the gated results at ED and ES (C and D). These two rows are both for 12.5-mm axial resolution. The bottom row shows gated results with high axial resolution (E and F).

compared between the following areas: the anterior free wall (sectors 6–8) and the antero-apical area (sectors 9–11); the antero-apical area and the anterior septum (sectors 12–14); and the anterior free wall and the antero-septum. Table 1 lists both the percent recovered activity (i.e., 100 implies an observed uptake which is 100% of the true activity concentration) for these three regions and the results of the statistical tests. The data were compared using a two-tailed paired Student's t test.

Figures 4A and B show ungated data for 7-mm in-plane resolution (PET) and 14-mm in-plane resolution (SPECT) respectively. A decrease, or local minimum, in recovered activity in the antero-apical area (sectors 9–11) is seen for both resolutions although it is statistically significant ($p < 0.05$) only for PET (Table 1). In addition, both show a significantly higher recovered activity in the anterior free wall (sectors 6–8) than in the septal sectors (12–14). From Table 1 the free wall and septal recovered activities were 85 and 76 respectively for PET and 65 and 55 for SPECT (both $p < 0.001$).

Figures 4C and D and Table 1 show the percent recovered activity at ED and ES for gated PET and SPECT scans (both with 12.5 mm axial resolution). The drop in counts in the antero-apical region persists at ED, becoming significant for SPECT as well as PET (both $p < 0.001$). However, this inhomogeneity is much less pronounced at ES, as shown in Table 1. In PET, for example, at ED the antero-apical and free wall activities are 69 and 84, respectively, and at ES they are 92 and 97, respectively. The free wall continues to have significantly higher measured activity than the septum at both ED and ES ($p < 0.001$ for both PET and SPECT, see Table 1). Again, this effect appears more pronounced at ED than at ES, especially for PET (Figs. 4C and D). At the higher axial resolution (i.e., for a scan which was subject to in-plane, but not axial, blurring), the free wall continues to have higher recovered activity than the septum at both ED and ES (both $p < 0.01$). However, the local minimum at the antero-apex is no longer apparent at ES for either PET or SPECT (Figs. 4E and F).

The data in Figure 4 and Table 1 show the average effects observed in the three adjacent slices (more apical, mid-ventricular and more basal). Nearly identical behavior was also observed in each of the three slices separately, although when taken alone each slice comprised a smaller data set and so the differences in activities were not always

TABLE 1
Recovered Activity as a Percentage of True Activity* Around the Myocardium

	PET Resolution			significance of difference between			SPECT Resolution			significance of difference between		
	Free wall	Antero-apex	Septum	Antero-apex and freewall	Antero-apex and septum	Free wall and septum	Free wall	Antero-apex	Septum	Antero-apex and freewall	Antero-apex and septum	Free wall and septum
Ungated	85 ± 7	72 ± 8	76 ± 6	<0.001	<0.05	<0.001	65 ± 7	54 ± 6	55 ± 7	<0.001	ns	<0.001
Gated												
Diastole	84 ± 10	69 ± 11	77 ± 9	<0.001	<0.001	<0.001	61 ± 11	48 ± 9	52 ± 8	<0.001	<0.001	<0.001
Systole	97 ± 2	92 ± 3	88 ± 9	<0.001	<0.02	<0.001	82 ± 4	76 ± 4	69 ± 8	<0.001	<0.001	<0.001
No axial blurring												
Diastole	88 ± 10	76 ± 11	83 ± 8	<0.001	<0.01	<0.01	63 ± 12	50 ± 10	54 ± 8	<0.001	<0.01	<0.001
Systole	99 ± 1	97 ± 2	93 ± 9	<0.01	<0.05	<0.01	84 ± 6	79 ± 6	71 ± 10	<0.01	<0.01	<0.001

*Mean ± s. d.
Freewall region = sectors 6–8, antero-apical region = sectors 9–11, septal region = sectors 12–14.

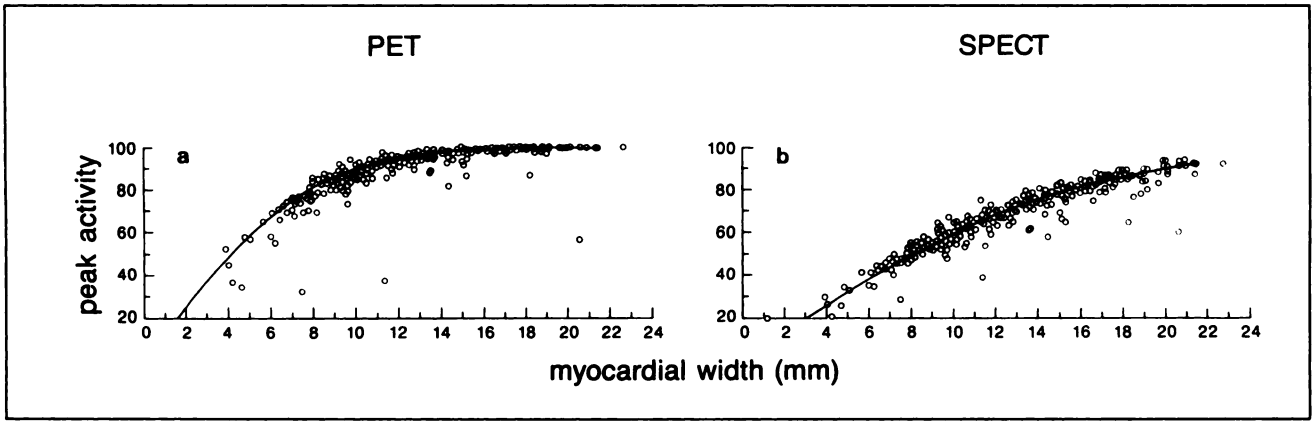

FIGURE 5. Percent recovered activity plotted against the corresponding myocardial thickness for each sector on high axial resolution MRI-based images, at both ED and ES. The left graph shows results for 7-mm in-plane resolution (PET) images. The right graph shows results for 14-mm in-plane resolution (SPECT).

significant. However, most of the general behavior described above can be seen qualitatively even in the images of the single subject shown in Figure 2—the free wall to septum ratio of greater than unity (which decreases towards unity at ES) and the antero-apical reduction in counts (which nearly disappears at ES).

Recovered Activity and Myocardial Thickness

Because the regional differences observed in Table 1 persisted for both good and poor axial resolutions, it was thought that the relationship between in-plane resolution and finite wall thickness might be a dominating factor. To investigate this possibility, the relationship between the percent recovered activity and the myocardial wall thickness, as determined from MRI, was examined. The thickness at each sector was computed from the transaxial MRI data using a two-dimensional version of the method of Beyar et al. (*9*). The percent recovered activity for each sector was plotted against the corresponding thickness, for each of the nine subjects, at both diastole and systole using the high axial resolution images (Fig. 5). The solid line shown on the graph is the predicted theoretical relationship between recovered activity and thickness, given the in-plane reconstructed resolution. In addition, the average thickness was calculated in each of the three regions around the myocardium. Table 2 gives these means and standard deviations and also significances of differences in thickness.

Patterns of Inhomogeneity in FDG Scans

Actual FDG scans were performed in five of the nine subjects. A central (mid-ventricular) slice was selected from each scan, and the myocardium was divided into 16 sectors, just as with the MRI-based data. It should be emphasized that this was not intended to be a definitive study of the normal myocardium in FDG imaging. However, it was felt that comparisons between the MRI-based studies and the corresponding actual FDG studies would be of interest. Table 3 (top row) shows the relative measured activity from the average of these five ungated FDG scans in the same three regions as were investigated for the MRI-based PET and SPECT scans. The FDG data were normalized so that for each subject that sector, the sector (of the 16 original sectors) with the highest activity was set to 100, prior to averaging all subjects together.

The first row of Table 3 shows a small but significant decrease in measured FDG activity in the antero-apical region, similar to the MRI-based data. However, the actual FDG scans show significantly higher counts in the anterior septum than in the anterior free wall–the opposite of the finding from the MRI-based data. It is not expected that the MRI-based PET data and the real FDG data agree, of

TABLE 2
Average Sector Width* Around the Myocardium

				Significance of difference between		
	Free wall	Antero-apex	Septum	Antero-apex and freewall	Antero-apex and septum	Free wall and septum
Diastole	11.5 ± 3.1	8.5 ± 2.1	8.8 ± 1.9	$p<0.001$	ns	$p<0.001$
Systole	17.4 ± 2.4	16.2 ± 1.9	13.7 ± 2.1	$p< 0.02$	$p < 0.001$	$p<0.001$

*Mean ± s.d. (mm).
Freewall region = sectors 6–8, antero-apical region = sectors 9–11, septal region = sectors 12–14.

TABLE 3
Measured Activity as a Percentage of Maximum Activity* Around the Myocardium

				Significance of difference between		
	Free wall	Antero-apex	Septum	Antero-apex and freewall	Antero-apex and septum	Free wall and septum
FDG	80 ± 10	78 ± 13	90 ± 5	ns	<0.05	<0.01
FDG corrected	98 ± 17	109 ± 20	115 ± 18	ns	ns	<0.01

*Mean ± s.d.
Freewall region = sectors 6–8, antero-apical region = sectors 9–11, septal region = sectors 12–14.

course, since the FDG data contain real physiologic variations, superimposed on the artifactual variations elucidated by the MRI-based images. Since these artifactual variations have already been computed for each of the five subjects, using the gated MRI data, it is obvious to ask how this information could be used to correct the measured FDG data for the artifactual variations. That is, how could the true, presumably physiologic, variations in FDG activity be measured?

To perform this calculation, the FDG value at each sector for each subject was divided by the percent recovered activity in that same sector, as obtained from the MRI data. The MRI and the FDG transaxial slices were previously aligned visually. This alignment, while crude, was estimated to be far more precise than the angular displacement of one sector while the three regions compared consisted of three sectors each.

The corrected FDG values are shown in the second row of Table 3. After correction, the antero-apical area no longer shows a local minimum in activity. Instead, there is a gradual increase in activity from anterior free wall to the antero-apical to the antero-septal regions. In addition, the free wall to septum ratio (computed from Table 3) is further magnified by the correction. In the raw data, the free wall to septum ratio was 80/90 = 0.89 (different from unity at $p < 0.01$). With correction, this ratio becomes 98/115 = 0.85 (different from unity at $p < 0.001$).

DISCUSSION

Artifactual variations in myocardial scans have been investigated on many previous occasions using animal models (*10*), phantoms (*11*) and human studies (*12,13*). These studies have shown that artifactual inhomogeneities in observed activity uptake can be caused by variations in wall motion or geometry or even by respiration. The importance of the partial volume effect in causing such artifacts in PET and SPECT images has been well established (*14*).

It is clear, therefore, that partial volume related effects can greatly influence the observed pattern of activity around the human myocardium. This means that a detailed understanding of the magnitude and origin of these artifacts is important for the proper interpretation of clinical scans. Using MRI-based images, it was possible to separate the effects of different sources of artifact: wall motion, axial resolution, variations in wall thickness, and in-plane resolution.

It should be noted that image noise was avoided by creating MRI-based images. All the effects described here would of course still be present to the same degree if noise were present. The only effect of noise would be to make measurement of small inhomogeneities more difficult.

Artifactual Inhomogeneities in Ungated Images

Two principal inhomogeneities were observed in the measured activity of ungated transaxial images (12.5 mm axial resolution): a depression of recovered activity in the antero-apical region and an erroneously increased value of recovered activity in the free wall compared to the septal wall. Since these results were derived from MRI-based images, the true activity ratio between any two regions around the myocardium is known to be unity. Comparison of single-sectors can therefore be used to demonstrate the magnitude of the artifacts. For example, if the antero-apical depression is described by comparing the minimum sector in the antero-apical region with the maximum sector in the septal region, the ratio for ungated images is 0.89 for PET and 0.92 for SPECT (see Figs. 4A and B). Both ratios differ significantly from unity ($p < 0.01$ and $p < 0.02$, respectively). Similarly, the free wall to septum ratio can be estimated by comparing single-sectors from Figure 4. In this case, the single-sector ratios were 1.12 for PET and 1.19 for SPECT, both differing from unity at $p < 0.001$.

Effect of Gating on Artifactual Inhomogeneities

The above information relates to ungated images. However, gated myocardial perfusion studies have been shown to be of value (*13,15*), so it is of interest to know the effect of gating on the uniformity of myocardial scans. To what extent is gating a useful tool in removing artifactual regional variations? To answer this question, we compared ungated with gated images. Both gated and ungated images had the same axial and in-plane resolution.

Compared with the ungated results, the gated images were more uniform at ES but much less uniform at ED (see Table 1 and Figs. 4C and D). This applied markedly in the case of the antero-apical depression, with the free wall to septum excess affected in a similar manner but to a lesser degree. Thus, the depression in antero-apical counts was

significantly worse at ED ($p < 0.02$ for both PET and SPECT), but essentially disappeared at ES. For example, with PET the single-sector apical/septal ratio was 0.82 at ED but much closer to unity (0.97) at ES (Figs. 4 C and D). Similarly, at diastole the free wall to septal ratio was not significantly changed for either PET or SPECT compared with the ungated images, while at systole it improved. For example, in Figure 4 the single-sector-to-freewall septal ratios at systole were 1.06 for PET (closer to unity than ungated, $p < .05$), and 1.14 for SPECT (closer to unity than ungated, p = ns).

From these results, it is clear that gating can effectively reduce artifactual inhomogeneities, but only in the ES images. ED images, in contrast, are markedly less uniform than the ungated images. It is interesting to note that in normal subjects, wall motion appears not to be a major cause of the observed inhomogeneities. If wall motion were a major contributing factor in the appearance of the artifacts, gated images would show more uniformity at both ED and ES than ungated images. This was very clearly not the case. Of course, it is possible that wall motion is more of a factor in subjects with wall motion abnormalities.

Relationship between In-plane Resolution and Myocardial Thickness

The relationship between wall thickness and in-plane resolution was investigated by comparing results at diastole and systole. Also important was the distribution of observed wall thicknesses (determined from MRI) and its relationship to count recovery at both PET and SPECT resolutions.

As noted above, ED images were less uniform than both ES images and ungated images. This suggests that wall thickness is very important in determining the degree of inhomogeneity in a myocardial scan. At ES, this observation is supported directly by the MRI wall thickness measurements which showed the same pattern around the myocardium as the recovered activity (Tables 1 and 2). That is, the wall thickness decreased in value from free wall to antero-apex to septum, with the apex and septum both significantly lower than the free wall. At ED, the mean wall thickness was again significantly higher in the free wall than in the septum. Also the antero-apical region showed a lower wall thickness than the septal region although not significantly so, presumably because of uncertainty in measuring wall width from the MRIs.

It is worth noting that, for PET resolution, ES changes in activity are much smaller than ED changes in activity (Figs. 4 C and E), even though the changes in thickness are comparable. This can be explained by examining Figure 5A which gives the relationship between thickness and recovered activity in a PET image. From this figure it can be seen that ES thicknesses fall on the part of the recovery–thickness curve with little or no slope. Hence, little variation in recovered activity occurs even with large variation in wall thickness.

For SPECT in-plane resolution, Figure 5 shows that the slope of the recovery–thickness curve is much lower at smaller thicknesses and more linear overall, without the initial steep slope and later plateau exhibited for PET data. The absence of the plateau for SPECT means that, even at systolic thicknesses, variations in thickness will cause variations in recovered counts. Thus the recovered activity shows much larger variations at systole for SPECT than for PET (Fig. 4). Also, for SPECT resolution, the variations in slope for smaller and larger thicknesses, although still present, are less dramatic. For this reason, the ED antero-apical depression is present but less marked in SPECT than in PET.

Effect of Axial Blurring on Artifactual Inhomogeneity

The effect of axial resolution on artifactual regional variation is also a matter of practical importance. This matter was addressed by comparing gated images that had been subject to axial blurring (i.e., 12.5 mm axial resolution) with those that had not. Both sets of images had identical in-plane resolution, so the only difference between the two sets was the presence or absence of axial blurring.

Removal of axial blurring (i.e., improving axial resolution) was found to have little or no effect on the uniformity of the images at both diastole and systole. For example, for PET the single-sector free wall to septum ratio at ED was 1.07 for high axial resolution and 1.10 for poor axial resolution (from Figs. 4C and E). Similarly, at ES, the single-sector free wall to septum ratios for PET were 1.03 and 1.06 for high and poor axial resolution, respectively. The effect of axial resolution is thus small, implying that typical machine to machine differences in axial resolution will make little difference in terms of minimizing these particular partial volume related artifacts in tomographic myocardial images. Of course, improved axial resolution may be advantageous for other reasons. For example, it should certainly improve detectability of small hot or cold lesions.

Correction of Artifactual Inhomogeneity in Myocardial Scans

As well as providing answers to questions about the relative importance of gating, axial resolution and in-plane resolution, the MRI-based images could in principle be used to correct clinical myocardial scans for artifactual nonuniformity. Some such correction is necessary if physiologic variations are to be identified with confidence. We emphasize that it was not our intent to use real FDG data to draw conclusions about physiologic inhomogeneities; the number of subjects is far too small. Further, the choice of matching slices in the MRI and FDG data sets was necessarily crude. The results presented here are therefore simply an example of how the MRI-based data could be used to correct actual FDG scans.

The measured, or uncorrected, FDG data showed the same pattern of apical depression as the MRI-based images, but the relationship of free wall to septal activity was reversed with higher activity in the septum than in the free wall (Table 3). After correction with the MRI data, the

normalized activity showed a steady rise from free wall to apex to septum. This suggests that, in these subjects, most or all of the observed antero-apical depression in measured FDG uptake is explicable as a partial volume artifact. In addition, the corrected free wall/septal ratio of less than unity suggests that partial volume effects, which elevate free wall activity over that in the septum, would tend to mask the real physiological variation in activity between these two regions. However, this inference is drawn from a very small number of subjects. Clearly, describing normal physiological variations in myocardial activity would require work beyond the purview of this paper.

CONCLUSION

Partial volume related inhomogeneities are known to affect tomographic scans of the myocardium. We have established that these artifactual variations can be substantially reduced by gating, but only in the case of the systolic image. The diastolic image is more inhomogeneous than the ungated image, because it is on average thinner. We also investigated axial blurring, but found that improvements in axial resolution have little effect on myocardial uniformity.

The most important factor for determining the degree of inhomogeneity in normal subjects was found to be the relationship between myocardial wall thickness and in-plane resolution, and not wall motion or axial resolution. This applies to both PET and SPECT resolutions, although the two in-plane resolutions lead to slightly different results given the range of thicknesses seen in normal myocardium. PET resolution is such that normal myocardial thickness at systole is generally sufficient to allow almost complete recovery of activity. However, the shape of the activity recovery versus wall thickness curve is more nonlinear for PET than for SPECT. Thus PET is more homogeneous than SPECT at end-systole but may be less so at end-diastole, depending on the range of myocardial wall thicknesses involved.

It was also possible to comment quantitatively on how partial volume artifacts affect the results of clinical studies of normal human myocardium. The range of wall thicknesses in normal subjects is such that partial volume effects will cause an artifactual increase in the free wall to septal activity ratio and a depression in the antero-apical activity. With gating, these inhomogeneities generally increase in ED images and decrease in ES images. Interpretation of myocardial images should take such artifactual variations into account.

REFERENCES

1. Baudhuin T, Melin JA, Marwick T, et al. Regional uptake and blood flow variations with N-13 ammonia in normal subjects do not correlate with flow or metabolic measurements by other methods [Abstract]. *J Nucl Med* 1992; 33:837.
2. Hicks RJ, Herman WH, Wolfe E, Kotzerke J, Kuhl DE, Schwaiger M. Regional variation in oxidative and glucose metabolism in the normal heart: comparison of PET-derived C-11 acetate and FDG kinetics [Abstract]. *J Nucl Med* 1990;31:774.
3. Gropler RJ, Siegel BA, Kenneth JL, et al. Nonuniformity in myocardial accumulation of fluorine-18-fluorodeoxyglucose in normal fasted humans. *J Nucl Med* 1990;31:1749–1756.
4. Kagaya Y, Kanno Y, Takeyama D, et al. Effects of long-term pressure overload on regional myocardial glucose and free fatty acid uptake in rats: a quantitative autoradiographic study. *Circulation* 1990;81:1353–1361.
5. Parodi O, Schelbert HR, Schwaiger M, Hansen H, Selin C, Hoffman EJ. Cardiac emission computed tomography: underestimation of regional tracer concentrations due to wall motion abnormalities. *J Comput Assist Tomogr* 1984;8:1083–1092.
6. Eisner RL, Schmarkey LS, Martin SE, et al. Defects on SPECT "perfusion" images can occur due to abnormal segmental contraction. *J Nucl Med* 1994;35:638–643.
7. Videen TO, Perlmutter JS, Mintun MA, Raichle ME. Regional correction of positron emission tomography data for the effects of cerebral atrophy. *J Cereb Blood Flow Metab* 1988;8:662–670.
8. Müller-Gärtner HW, Links JM, Prince JL, et al. Measurement of radiotracer concentration in brain gray matter using positron emission tomography: MRI-based correction for partial volume effects. *J Cereb Blood Flow Metab* 1992;12:571–583.
9. Beyar R, Shapiro EP, Graves WL, et al. Quantification and validation of left ventricular wall thickening by a three-dimensional volume element magnetic resonance imaging approach. *Circulation* 1990;81:297–307.
10. Gewirtz H, Grotte GJ, Strauss HW, et al. The influence of left ventricular volume and wall motion on myocardial images. *Circulation* 1979;59:1172–1177.
11. Galt JR, Garcia EV, Robbins WL. Effects of myocardial wall thickness on SPECT quantification. *IEEE Trans Med Imag* 1990;9:144–150.
12. Haronian HL, Sinusas AJ, Remetz MS, et al. Effects of altered left ventricular geometry on quantitative technetium 99m sestamibi defect size in humans: perfusion imaging during coronary angioplasty. *J Nucl Cardiol* 1994;1:150–158.
13. Ter-Pogossian MM, Bergmann SR, Sobel BE. Influence of cardiac and respiratory motion on tomographic reconstructions of the heart: implications for quantitative nuclear cardiology. *J Comput Assist Tomogr* 1982;6: 1148–1155.
14. Hoffman EJ, Huang S-C, Phelps ME. Quantitation in positron emission computed tomography: I. Effect of object size. *J Comput Assist Tomogr* 1979;3:299–308.
15. Hoffman EJ, Phelps ME, Wisenberg G, Schelbert HR, Kuhl DE. Electrocardiographic gating in positron emission computed tomography. *J Comput Assist Tomogr* 1979;3:733–739.